Electromechanical System-in-Package Carbon Nanotube VCO

Christian Kauth, Marc Pastre, and Maher Kayal

***Abstract*—Encapsulated tunable electromechanical oscillators are a milestone on the road to smart dust sensor nodes. To foster the advent of ultrahigh system sensitivity thanks to novel technologies, a computationally light analytical and semi-empirical model for carbon nanotube resonator dynamics, electromechanical and piezoresistive properties is presented. This model is the breeding ground for the subsequent design and integration of a phase locked loop and feedback circuitry, which form an adaptive closed-loop oscillator for actuation, detection and sustainment of the nanotube's motion. Closed-loop operation and tube stretching make the system widely universal and invariant to spreads in nanotube characteristics.**

***Index Terms*—Analytical models, Carbon nanotubes, Circuit analysis, Closed loop systems, Nanoelectromechanical systems, Oscillators, Phase locked loops.**

I. Introduction

SMART dust sensor systems take advantage of the subtle sensing capabilities of nanomechanical devices, the versatile functionalities available in electronics, sophisticated processing algorithms and hybrid packaging techniques. The static operation sensitivity of such sophisticated micro- and nanoelectromechanical systems (NEMS) is boosted by their intrinsic quality factor Q in dynamic operation modes and lead to the development of transducers that actuate and sense mechanical phenomena via electrical signals. Appropriate actuation and detection design strongly depends on the electrical and mechanical properties of the NEMS, which may be only partially controllable or unpredictable, especially for experimental non-silicon technologies. Suspended carbon nanotubes (CNT-NEMS) are such low-mass, highly sensitive sensors, whose electromechanical properties strongly depend on length, diameter, chirality, defect rate, placement and bias. As these parameters may alter considerably from one device to another, and given that signals are feeble, the actuation and detection circuitry has to be tuned from case to case, a working approach only as long as yield remains unconsidered. Though successful open-loop operation of CNT-NEMS has been reported [1], [2], closed-loop circuits that automatically adapt to the CNT-NEMS properties are still in the fledgling stages [3] and would benefit from a lightweight NEMS and circuit model, reflecting the electrical and mechanical properties.

This contribution presents a systematic approach for closed-loop NEMS oscillator circuit design, based on the omnipresent piezoresistive property of CNT-NEMS [4]. An overview of the system architecture is provided in section II, before the relevant dynamics and electromechanical transduction principles of carbon nanotube resonators are analysed, quantified and modelled in section III. Motional information processing is the topic of section IV and leads to a closed-loop oscillator feedback design in section V, where the previously developed models condensate into circuitry and are validated via measurements. CMOS circuit integration follows in section VI and the compatibility between the circuit and NEMS is finally assessed in section VII.

All authors are with the Electronics Laboratory, Ecole Polytechnique Fédérale de Lausanne, CH-1015, Switzerland (see http://elab.epfl.ch).

II. System Architecture

The packaged sensor die, shown in Fig. 1a, consists of a NEMS chip with a locally grown CNT resonator [5], connected to the CMOS chip, hosting the control circuitry, by through silicon vias (TSV). A glass cap, potentially equipped with a getter or gas inlet, defines the sensed environment. The 3D-integration process is detailed in [6] and assembles the silicon CMOS and silicon-on-insulator NEMS chips by a stud bump technology, while the glass cap is eutectically bonded to the latter. Ohmic contacts and TSVs resisting CNT growth temperature [6] combine into a feasible process flow.

The CNT-NEMS is conceptually embedded into a phase locked loop (PLL), exhibited in Fig.1b, formed by a phase frequency detector (PFD), a loop filter (LF) and a voltage controlled oscillator (VCO), that detects and maintains the NEMS motion at a frequency defined by the loop phase $\Delta\Phi$ and the NEMS' eigenfrequency. The latter is sensitive to the environment and shifts when a particle binds onto the CNT-NEMS, which enables sensor operation of the proposed topology. Further does an actuator enable frequency tuning by straining the CNT-NEMS, as Fig.1c shows. The suspended CNT is electrostatically actuated by the nearby gate (G) electrode and motion is inferred from source (S) drain (D) current modulation.

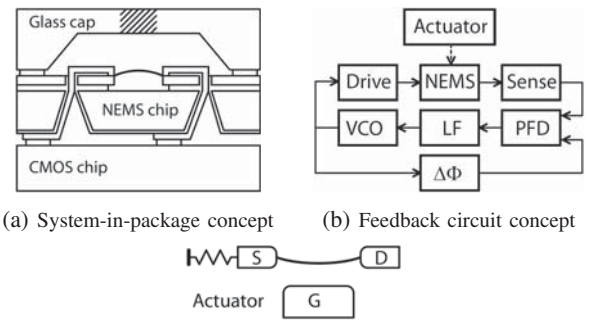

(a) System-in-package concept (b) Feedback circuit concept

(c) CNT-NEMS terminals

Fig. 1. System architecture

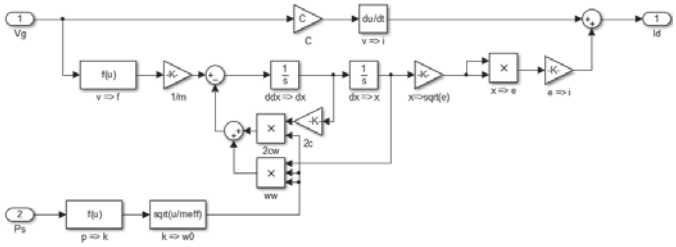

Fig. 2. Piezoresistive and capacitive CNT-NEMS model for Simulink

III. Piezoresistive CNT NEMS Resonator Model

The CNT is suspended over a trench and a nearby electrode, allows for its actuation by exerting an electrostatic force created via application of a voltage V on the two-port capacitor formed by the electrode and the CNT. Neglecting the effect of the density of states in the CNT and approximating the NEMS as a long equipotential cylinder above an infinite plate, derivation of the system energy with respect to position yields the force

$$F(t) = \frac{V(t)^2 \pi \epsilon_0 L}{h \operatorname{arccosh}^2\left(\frac{h}{r}\right)} \tag{1}$$

where the tube radius r and displacement are considered inferior to the suspension height h. L is the length of the CNT and ϵ_0 the vacuum permittivity.

The tube's motion is to be inferred by sensing the piezoresistive modulation of the current through the tube, caused by the latter's periodic elongation when vibrating. This current's frequency informs about the mechanically sensed phenomena, and together with the phase, it shall be tracked to sustain the oscillation. From a system perspective, the dynamics of the oscillator's core component may be satisfactorily described as a driven harmonic oscillator balancing the driving, restoring and frictional forces, with parameters extracted from empirical data, that is

$$\partial_t^2 \hat{x} + 2\zeta\omega_0 \partial_t \hat{x} + \omega_0^2 \hat{x} = \frac{1}{m_{\text{eff}}} F(t) \tag{2}$$

where $\hat{x}$ is the oscillation half-amplitude, $\zeta = \frac{1}{2Q}$ the damping ratio, m_{eff} the CNT's effective mass, $F(t)$ the actuating force and ω_0 the NEMS eigenfrequency

$$\omega_0 = 2\pi \sqrt{\frac{E}{3\rho L^2}\left(\frac{\pi^2 r^2}{L^2} + \frac{\Delta L}{L}\right)} \tag{3}$$

when defining ρ as the CNT density, E its Young modulus, L the tube length at rest and ΔL its elongation induced by pulling via an actuator (see Fig. 1c and section VII) and approximating the CNT mode shape by [7]

$$x(l,t) = \frac{\hat{x}(t)}{2}\left(1 - \cos\left(\frac{2\pi l}{L}\right)\right) \quad , \quad l \in [0..L] \tag{4}$$

For a sinusoidal driving force $F_0 \sin(\omega t)$, equation (2) has a transient solution with exponential decay time constant $\tau = \frac{1}{\zeta\omega_0}$ and a permanent solution

$$\hat{x}(t) = \frac{F_0}{m_{\text{eff}} Z_m \omega} \sin(\omega t + \phi) \tag{5}$$

TABLE I
Experimental order of magnitude for model parameters

Parameter	Symbol	Value	Unit	Source
Length	L	1	μm	[1], [2]
Radius	r	1	nm	[1], [2]
Height	h	1	μm	[1], [2]
Damping	ζ	1/100	-	[1]
Bias	I_0	1	μA	[4]
Gauge factor	β	100	-	[4]
Effective mass	m	6.6	ag	
Eigenfrequency	ω_0	40	MHz	
Coupling	C	100	aF	

where $Z_m = \sqrt{(2\omega_0\zeta)^2 + \frac{1}{\omega^2}(\omega_0^2 - \omega^2)^2}$ is the motional impedance and $\phi = \arctan\left(\frac{2\omega\omega_0\zeta}{\omega^2 - \omega_0^2}\right)$ the phase delay with respect to the drive signal, if taken in $[-\pi; 0]$. This entails a resonance frequency at $\omega_r = \omega_0\sqrt{1 - 2\zeta^2}$ if the damping is smaller than $\zeta < \frac{1}{\sqrt{2}}$. The displacement induces a strain of

$$\epsilon(t) = \left(\frac{\pi}{2L}\hat{x}(t)\right)^2 \tag{6}$$

when modelling the CNT shape by equation (4) and applying a Taylor expansion during arc length evaluation. Supposing a linear dependence of the CNT resistance on the induced strain and a constant piezoresistive gauge factor β [4], the piezoresistive current modulation writes

$$\delta I_{piezo}(t) = I_0 \beta \epsilon(t) \tag{7}$$

where I_0 is the CNT bias current. This piezoresistive current is obfuscated by the direct capacitive coupling through the capacitor C, formed by the detection and actuation electrodes, expressed by

$$\delta I_{capa}(t) = C\omega V(t) \tag{8}$$

Table I populates the precedent formulas with orders of magnitude extracted from empirical data, which constitutes a very practical approach to generate a model which interpolates reality to its best.

Simulating the model's implementation in Simulink (see Fig. 2), instantiated with the values of Table I, for which the transient response decays with $\tau = 400$ ns, yields the frequency responses of Fig. 3. For a driving voltage of $\frac{1}{\sqrt{2}}$ V, the oscillation amplitude reaches 30 nm, which corresponds to an

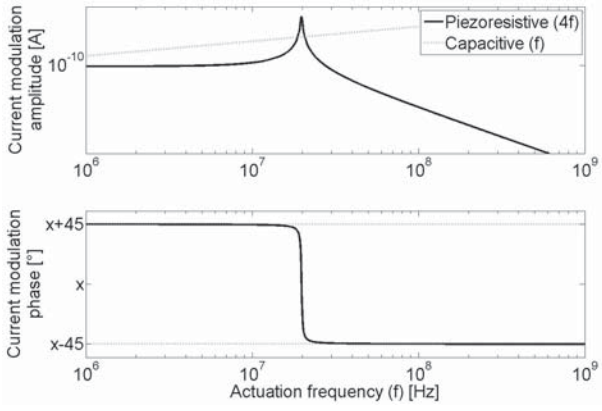

Fig. 3. Frequency response of CNT-NEMS for values of Table I

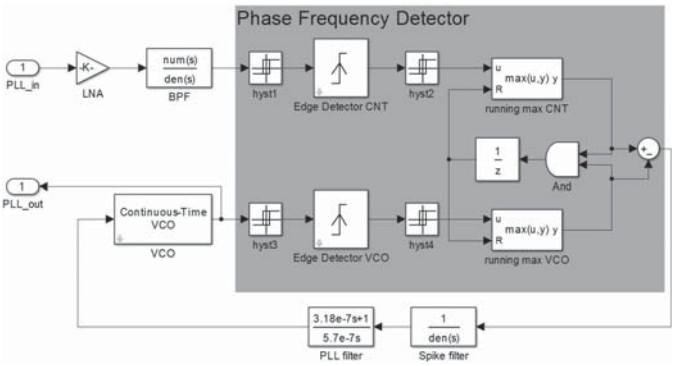

Fig. 4. PLL model for Simulink

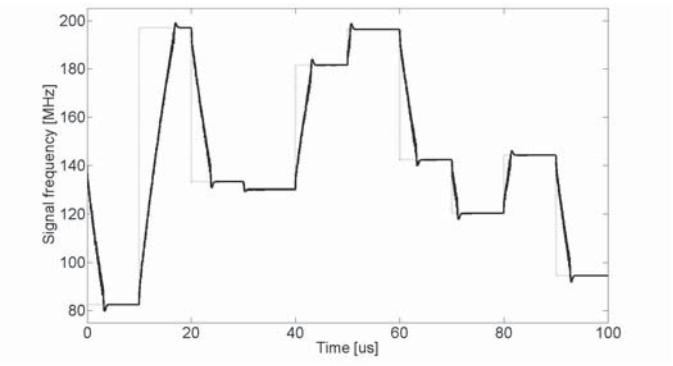

Fig. 5. PLL tracking of random frequency jumps by CNT-NEMS

induced strain of 0.2 % and a piezoresistive current modulation exceeding tens of nA near and hundreds of nA at resonance, which occurs for an actuation at half the eigenfrequency, in accord with (1). The piezoresistive Lorentzian stands out of the capacitive feedthrough only for drive frequencies close to resonance. Isolation of the motional information can nevertheless be retrieved via filtering, as the two components occur at different frequencies - once and four times the driving frequency for the capacitive and piezoresistive components respectively. After division, the frequency-dependent phase of equation (5) spans 90° of the actuating signal's period and any feedback circuit's phase shall complement the NEMS' phase to a multiple of 180° of the actuating signal's period. It is noteworthy that the electrostatic force is purely attractive and consequently invariant to the signal's sign, or equivalently, to a 180° phase shift of a zero-centered sinus.

IV. Signal Isolation

This piezoresistive signal can be read out of the NEMS via a low-noise front-end (LNA) [8], amplified and filtered with respect to the capacitive feedthrough before it enters the feedback loop. The detected signal could, after some processing, indeed actuate the NEMS directly to sustain the oscillation. This approach requires some amplitude control to avoid dynamic pull-in and subsequent destruction of the NEMS structure via positive amplitude feedback. For this reason and for the convenience of testing the circuitry in absence of a CNT-NEMS, a different approach is adopted. A Phase Locked Loop (PLL) is designed, whose frequency is imposed by the NEMS. An internal voltage controlled oscillator (VCO) locks on the CNT's phase and ensures steady amplitude-independent actuation.

The PLL consists of a phase- and frequency-detector (PFD) block, a loop filter and a local VCO (see Fig. 4).

- The PFD detects rising edges of the two tracks, the CNT and VCO outputs. If such an edge is detected, the internal signal of the respective track goes to logical one. As soon as both signals are high, they are reset instantly. This yields on the long signals whose high-time is proportional to their phase advance with respect to the other. Their subtraction is then a square signal that is positive when the VCO leaks phase, negative when it has phase advance, and has a time-average value proportional to the phase difference, with proportionality factor K_ϕ.

$$V_{\text{PFD}}(s) = K_\phi\left(\phi_{\text{CNT}}(s) - \phi_{\text{VCO}}(s)\right) \tag{9}$$

  This way of detecting phase and frequency allows to follow frequencies over the complete spectrum.
- The VCO generates a frequency K_V-proportional to its steering voltage,

$$\omega_{\text{VCO}}(s) = K_V F(s) V_{\text{PFD}}(s) \tag{10}$$

  where $F(s)$ is the filter transfer function. The phase being the integral of the angular frequency, equations (9) and (10) combine into

$$\frac{\phi_{\text{VCO}}}{\phi_{\text{CNT}}} = \frac{\omega_{\text{VCO}}}{\omega_{\text{CNT}}} = \frac{1}{1 + \frac{s}{K_V K_\phi F(s)}} \tag{11}$$

- The loop filter has to average the PFD's output. A first-order integrator filter (LF)

$$F(s) = \frac{1 + \tau_2 s}{\tau_1 s} \tag{12}$$

  allows to follow phase and frequency jumps, as follows from the substitution of (12) in (11)

$$\frac{\phi_{\text{VCO}}}{\phi_{\text{CNT}}} = \frac{\omega_{\text{VCO}}}{\omega_{\text{CNT}}} = \frac{1 + s\frac{1}{\omega_n Q}}{1 + s\frac{1}{\omega_n Q} + s^2\frac{1}{\omega_n^2}} \tag{13}$$

  where the natural loop frequency and quality factor are $\omega_n = \sqrt{\frac{K_V K_\phi}{\tau_1}}$ and $Q = \sqrt{\frac{\tau_1}{K_V K_\phi}}\frac{1}{\tau_2}$.

Given the NEMS parameters from section III, a natural loop frequency of 1 MHz is chosen and critical damping is achieved for $Q = 1/2$ to converge as fast as possible without oscillating. The tracking and locking behaviour of the PLL is simulated in Fig. 5, for which the parameter set of real components, as

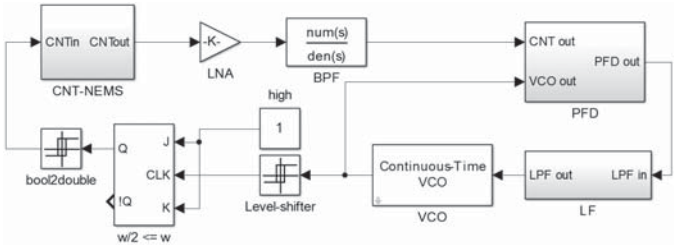

Fig. 6. Digital closed-loop CNT-NEMS oscillator model for Simulink

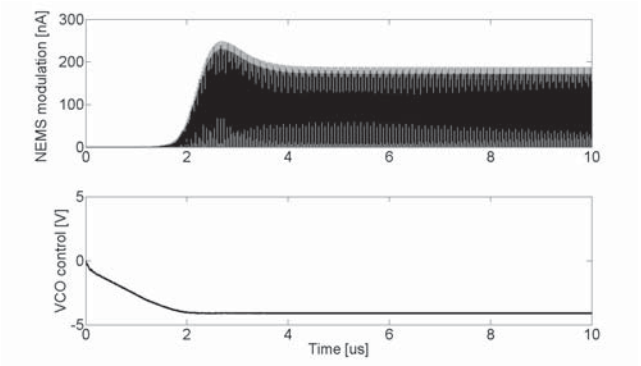

Fig. 7. Oscillation build-up for system in closed-loop configuration

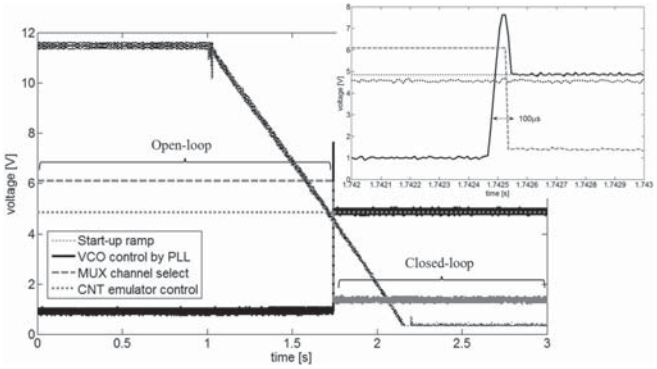

Fig. 9. Measurement of start-up sweep and automatic lock detection

presented in section V, has been used. That PLL has a free-running frequency of 140 MHz and can be tuned by 15 MHz per volt over a ± 4 V range. The frequency jumps of the CNT corresponding to molecular binding or release in sensor applications, can be tracked within a 10 μs time lap.

V. Oscillator Design and Implementation

The feedback loop on the NEMS is then closed by dividing the VCO signal by four for sinusoidal actuation, or by two for square actuation, as suggested by equations (1) and (6). The square actuation circuit is depicted in Fig. 6, while the VCO steering signal as well as the current modulation through the NEMS are subject of Fig. 7. The NEMS start-up suffers a latency caused by the parasitic information carried by the capacitive feedthrough, which is considerably larger for square actuation. If this is considered to be an issue, it can be countervailed by more aggressive filtering in the bandpass filter (BPF) following the LNA, or by limiting the slew-rate of the NEMS actuation stage. The VCO steering signal settles slightly below -4V, corresponding to an oscillation frequency of 80 MHz, which is required to actuate the NEMS at its eigenfrequency (see Table I) after frequency division via a J-K flip-flop. At steady state, the CNT signal lost part of its peak amplitude. This is due to the feedback loop delay, which causes an additional phase shift and makes the CNT resonate at a frequency, close to its eigenfrequency, where an overall closed-loop phase congruent modulo 180° is achieved (see Fig. 3).

The NEMS is not expected to yield a detectable signal when merely driven by thermal noise, making a start-up circuit indispensable for practical applications. This one consists of a voltage ramp sweeping the VCO through decreasing frequencies. Its practical operation is illustrated in Fig. 9. As long as the frequency is above the NEMS resonance, no signal is detected by the LNA, and the floating LF output indicates phase advance of the VCO. Once the drive approaches the NEMS' eigenfrequency, a signal is detected from the NEMS, which is compared with the steadily decreasing VCO frequency. The LF output changes polarity to indicate that the VCO now leaks phase. This edge is used to trigger a lock detector, which switches the multiplexer (MUX) from the start-up ramp to the LF output and hence closes the oscillator loop, which now continues working according to the principles highlighted above. The complete topology is shown in Fig. 10 and the shaded area has been implemented on an FR-4 printed circuit board (PCB), which contains additionally a CNT-NEMS emulator, so that loop functionality could be tested and verified with an onboard test signal. The chosen PFD has unlimited capture range and its voltage excursions of twice 750mV must cover 360° of phase advance or delay, resulting in a PFD gain of $K_\phi = 239\frac{\text{mV}}{\text{rad}}$. The inductance and tunable capacitance in the VCO's LC tank were chosen to cover a frequency range from 80 MHz to 200 MHz via a 8 V control voltage excursion, which translates into a VCO gain of $K_V = 15\ \frac{\text{MHz}}{\text{V}}$. The LF has been implemented as a differential active first-order integrator and the RC time-constants for equation (12) were chosen as $\tau_1 = \frac{K_V K_\phi}{\omega_n^2}$ and $\tau_2 = \frac{1}{Q\omega_n}$.

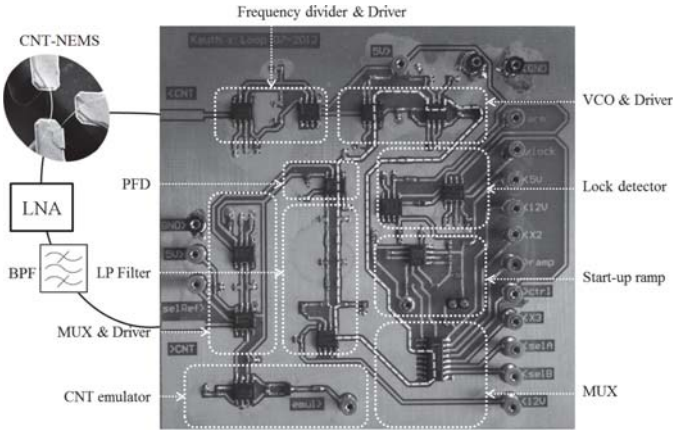

Fig. 8. PCB implementation of the feedback loop (PLL path appears dashed)

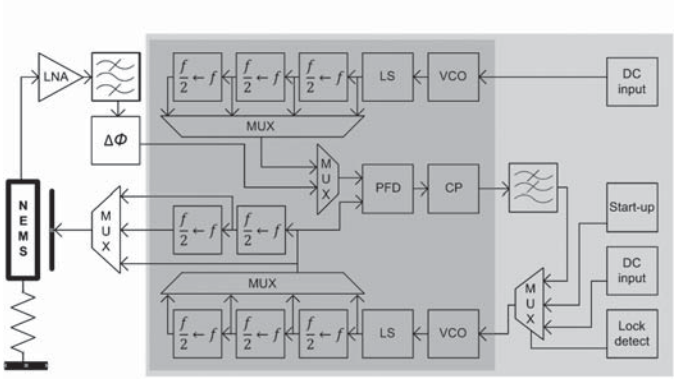

Fig. 10. Closed-loop topology for CNT-NEMS oscillator

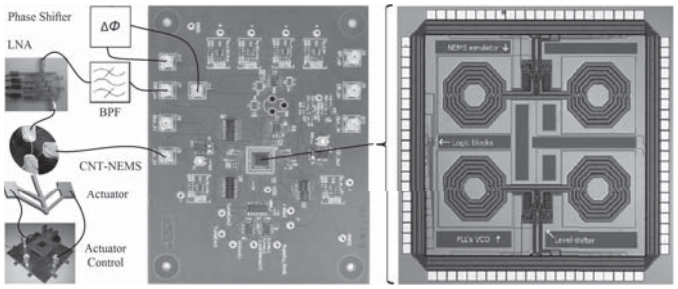

Fig. 11. Partially integrated voltage controlled CNT-NEMS oscillator

An additional pole is integrated into the LF at 5 ω_n to inhibit the pulse transients while causing acceptable further overshoot. Finally the start-up ramp is generated with a Deboo integrator for unipolar non-inverting designs, based on a Howland current source [9]. The excursion covers 12 V within 1.2 s, which is considerably slower than the loop settling time and allows resonance to build up properly. These values from real components have also been used in the previous simulations. This implementation is adequate for oscillators around CNT-NEMS that have eigenfrequencies in the 40 MHz to 100 MHz range. Adaptation of the range to lower frequencies is uncomplicated and achieved by replacing the inductor of the LC tank, while higher ranges are inaccessible due to frequency limitations of the PCB components and require integration of the circuit [10].

VI. CMOS Integration

A first integration step followed the proof of concept delivered by the previously presented PCB circuit implementation. Integrated in a 180nm CMOS technology were first and foremost the sensible high frequency blocks forming the PLL (indicated by the dark grey area of Fig. 10). The resulting 4.5mm^2 chip hosts two 3-bit programmable LC-tank VCOs, one for the PLL, the other as a NEMS emulator, able to span frequencies from 600MHz to 771MHz (see Fig. 12), a frequency range sufficiently high to integrate the inductor coil with reasonable surface overhead, and low enough to prevent challenging RF layout issues. Level-shifters saturate the sinusoidal VCO signal into a digital signal and frequency dividers allow to extend the operation range of the chip to the 300MHz-385MHz, 150MHz-192MHz and 75MHz-96MHz bands. The union of these frequency ranges covers a considerable part of the CNT-NEMS oscillation spectrum, and may address even

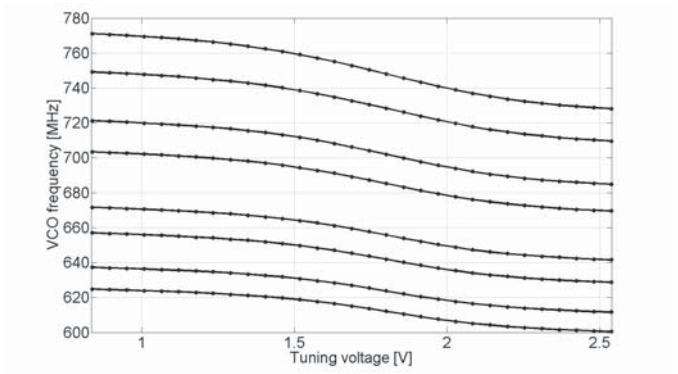

Fig. 12. Measured integrated VCO transfer characteristic

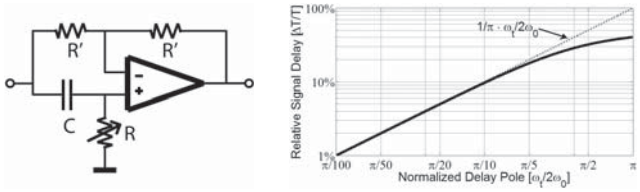

(a) Phase shifter $T(s)$ (b) Controllable phase shift

Fig. 13. Adjustable loop delay

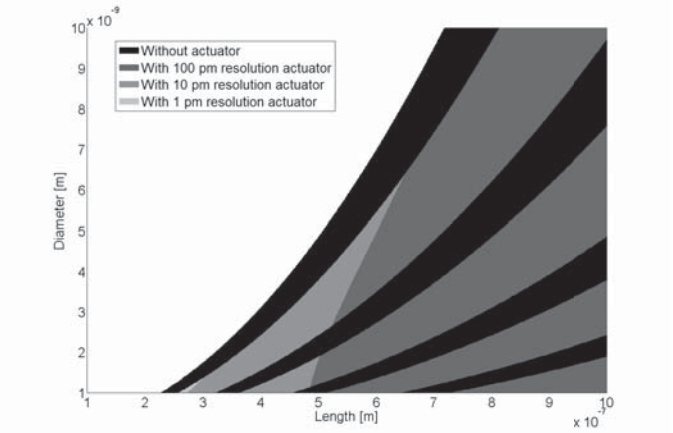

Fig. 14. CNT-NEMS device space compatible with presented IC circuitry

more CNT-NEMS resonators thanks to the actuator, as will be shown in section VII. The detailed chip description may be looked-up in [10]. Worth mentioning are the three chip outputs that allow to drive the CNT-NEMS at a quarter, half and full its electrical signal frequency, meaning that field-effect and piezoresistive phenomena may be exploited in the oscillator, as explained in [11]. The loop filter has been kept off-chip at this stage, in order to allow flexible tuning of the system dynamics [12]. The piecewise integrated system is shown in Fig. 11 and is composed of a PCB hosting the integrated circuit (IC), the PLL filter, start-up and lock-detection blocks, as well as current and voltage references. A microcontroller controls the actuator that strains the CNT-NEMS in order to oscillate at the desired frequency, which makes this system a voltage controllable electromechanical oscillator. The NEMS motion is read by a low-noise amplifier [8] and the motional information extracted by the bandpass filter, briefly addressed in [11]. Best signal strength out of the CNT-NEMS is obtained when the loop phase $\Delta\Phi$ is set in accord with the electronic block delays, to make the NEMS oscillate close to its eigenfrequency, where it exhibits a $\frac{\pi}{2}$ phase shift. This delay in the signal path may be generated by a long cable, a programmable counter, or the phase shifter of Fig. 13

$$T(s) = \frac{\frac{s}{\omega_t} - 1}{\frac{s}{\omega_t} + 1}, \text{ with } \omega_t = \frac{1}{RC} \tag{14}$$

that delays the piezoresistive signal with frequency $2\omega_0$ by $2\arctan\left(\frac{2\omega_0}{\omega_t}\right) \approx 4\frac{\omega_0}{\omega_t}$ with no impact on the amplitude $|T(s)|$=1.

VII. NEMS vs. Circuit Compatibility

In order to assess the potential of joint CNT-NEMS and IC operation, the NEMS eigenfrequency (3) for common CNT dimensions is compared to the available IC bands. Recalling that the piezoresistive current modulation in CNT-NEMS is quasi omnipresent and appears at twice the NEMS oscillation frequency (6), the presented IC may sustain piezoresistive oscillation of CNT-NEMS with eigenfrequencies in the 38MHz-48MHz, 75MHz-96MHz, 150MHz-192MHz and 300MHz-385MHz ranges. Adequate CNT dimensions for those bands are indicated in black in Fig.14.

The compatibility of the IC to a wider region of the CNT parameter space may be achieved by the use of a MEMS actuator and a set of levers to strain the CNT by pulling its source (see Fig. 1c) and consequently tuning its eigenfrequency (3) to bands accessible to the IC. While thermal and electrostatic actuators may be obtained with CMOS compatible integration processes, their displacement resolution in the order of 10nm is insufficient for tuning purposes. But picometer displacement may be obtained with magnetic or piezoelectric actuators [13], in combination with a lever, and would substantially extend the joint CNT-NEMS and IC compatibility range. The price to pay for this compatibility enhancement comes with considerable challenges at the NEMS integration process level.

VIII. Conclusion

An analytic model for piezoresistive carbon nanotube electromechanical resonators has been presented and was fed with empirically deduced data to model the sensor's transfer function. The development of an analytical solution and its computational ease promoted the design and simulation of a phase locked loop, isolating and tracking the motional information from the sensor. The system has been implemented on a printed circuit board and was proven to correctly operate on an emulated version of the NEMS with eigenfrequencies in the 40 MHz to 100 MHz range. Integration of the phase locked loop in a 180nm technology forms a first step towards smart dust system-in-package sensors. The additional use of an integrated MEMS actuator allows to tune the carbon nanotube's operation frequency, opening the gate to voltage controllable electromechanical oscillator applications, and enhancing the compatibility between circuit and sensor.

Acknowledgment

This research has been funded by Nano-Tera.ch, a program of the Swiss Confederation, evaluated by SNSF.

References

[1] V. Sazonova, Y. Yaish, H. Ustunel, D. Roundy, T. A. Arias, and P. L. McEuen, "A tunable carbon nanotube electromechanical oscillator," *Nature*, vol. 431, no. 7006, pp. 284–287, Sep. 2004.

[2] H. Peng, C. Chang, S. Aloni, T. Yuzvinsky, and A. Zettl, "Ultrahigh frequency nanotube resonators," *PRL*, vol. 97, p. 087203, Aug 2006.

[3] C. Kauth, M. Pastre, and M. Kayal, "Closed-loop oscillator circuit for piezoresistive carbon nanotube nems resonators," *Mixed Design of Integrated Circuits and Systems conference proceedings*, pp. 365–368, June 2013.

[4] T. Helbling, "Carbon nanotube field effect transistors as electromechanical transducers," *http://dx.doi.org/10.3929/ethz-a-006054786*, 2010.

[5] M. Ishida, H. Hongo, F. Nihey, and Y. Ochiai, "Diameter-controlled carbon nanotubes grown from lithographically defined nanoparticles," *Jpn. J. Appl. Phys.*, vol. 43, p. 1356, 2004.

[6] R. Gueye, S. W. Lee, T. Akiyama, D. Briand, C. Roman, C. Hierold, and N. F. de Rooij, "High-temperature compatible 3d-integration processes for a vacuum-sealed cnt-based nems," p. 86140H, 2013.

[7] H. Postma, I. Kozinsky, A. Husain, and M. L. Roukes, "Dynamic range of nanotube- and nanowire-based electromechanical systems," *Applied Physics Letters*, vol. 86, no. 22, pp. 223 105 –223 105–3, may 2005.

[8] C. Kauth, M. Pastre, and M. Kayal, "Wideband low-noise rf front-end for cnt-nems sensors," *Mixed Design of Integrated Circuits and Systems conference proceedings*, pp. 289–293, May 2012.

[9] G. J. Deboo, "A novel integrator results by grounding its capacitor," *Electronic Design*, vol. 15, 1967.

[10] C. Kauth, M. Pastre, and M. Kayal, "A self-regulating oscillator for sensor operation of nanoelectromechanical systems," *New Circuits and Systems conference proceedings*, pp. 1–4, June 2013.

[11] C. Kauth, M. Pastre, J. Sallese, and M. Kayal, "System-level design considerations for carbon nanotube electromechanical resonators," *Journal of Sensors*, vol. in press, 2013.

[12] C. Kauth, M. Pastre, and M. Kayal, "Robust control of oscillating nems sensors," *IEEE International Conference on Electronics, Circuits and Systems*, accepted (United Arab Emirates / Abu Dhabi), December 2013.

[13] D. Bell, T. Lu, N. Fleck, and S. Spearing, "Mems actuators and sensors: observations on their performance and selection for purpose," *J. Micromech. Microeng.*, vol. 15, pp. 153–164, 2005.

Christian Kauth received the B.S. in electrical engineering from Ecole Polytechnique Fédérale de Lausanne (EPFL, Switzerland) in 2007 and a joint M.S. in micro- and nanotechnologies for integrated systems from EPFL, Politecnico di Torino (POLITO, Italy) and the Grenoble Institute of Technology (INP, France) in 2009. He currently is about to complete the Ph.D. degree at EPFL with research interests in carbon nanotube physics, microelectromechanical systems, sensor interfaces, oscillator design, analog circuits and algorithms. Next he will join Microsoft (Seattle, USA) as a software development engineer

Marc Pastre received the B.S. and M.S. degrees in computer science and the Ph.D. degree in microelectronics from the Ecole Polytechnique Fédérale de Lausanne (EPFL, Switzerland) in 2000 and 2005 respectively. His research interests include low-power analog and mixed-signal circuits, ADCs/-DACs, high-performance sensor interfaces, digital enhancement of analog circuits and CAD tools.

Maher Kayal received M.S. and Ph.D degrees in electrical engineering from the Ecole Polytechnique Fédérale de Lausanne (EPFL, Switzerland) in 1983 and 1989 respectively. He has been with the Electronics laboratories of EPFL since 1990, where he is currently a professor and director of the "Energy Management and Sustainability" section. He has published many scientific papers, coauthor of three text books dedicated to mixed-mode CMOS design and he holds seven patents. His technical contributions have been in the area of analog and Mixed-signal circuits design including highly linear and tunable sensors microsystems, signal processing and green energy management. He received the Swiss Ascom award in 1990 for the best work in telecommunications and the Swiss Credit best teaching award in 2009.